

Fatigue properties of rolled AZ31B magnesium alloy plate

S. MORITA¹, N. OHNO¹, F. TAMAI², Y. KAWAKAMI²

1. Faculty of Science and Engineering, Saga University, Saga 840-8502, Japan;

2. Material and Environment Department, Industrial Technology Center of Saga, Saga 849-0932, Japan

Received 23 September 2009; accepted 30 January 2010

Abstract: Fatigue strength, crack initiation and propagation behavior of rolled AZ31B magnesium alloy plate were investigated. Axial tension–compression fatigue tests were carried out with cylindrical smooth specimens. Two types of specimens were machined with the loading axis parallel (L-specimen) and perpendicular (T-specimen) to rolling direction. Monotonic compressive 0.2% proof stress, tensile strength and tensile elongation were similar for both specimens. On the other hand, monotonic tensile 0.2% proof stress of the L-specimen was slightly higher than that of the T-specimen. Moreover, monotonic compressive 0.2% proof stresses were lower than tensile ones for both specimens. The fatigue strengths of 10^7 cycles of the L- and T-specimens were 95 and 85 MPa, respectively. Compared with the monotonic compressive 0.2% proof stresses, the fatigue strengths were higher for both specimens. In other words, the fatigue crack did not initiate and propagate even though deformation twins were formed in compressive stress under the cyclic tension–compression loading. The fatigue crack initiated at early stage of the fatigue life in low cycle regime regardless of specimen direction. The crack growth rate of the L-specimen was slightly lower than of the T-specimen. Consequently, the fatigue lives of the L-specimen were longer than those of the T-specimen in low cycle regime.

Key words: magnesium alloy; compressive proof stress; fatigue strength; crack initiation; crack propagation

1 Introduction

Magnesium alloys are the lightest structural materials with high specific strength and stiffness. Therefore, this advantage makes magnesium alloys attractive for the automobile and aircraft industry[1–2]. It is necessary to investigate the cyclic loading behavior, especially high cycle fatigue properties for use of structural parts. It is well known that magnesium and its alloys have a hexagonal close-packed (HCP) structure and strong texture formed by processing. In polycrystalline magnesium alloys, basal planes are distributed parallel to extrusion direction by extrusion processing. On the other hand, basal planes are aligned parallel to rolling direction by rolling processing. Depending on the HCP structure and strong texture, deformation twins easily form when the material is subjected to compressive stress in loading direction parallel to extrusion direction at room temperature. This behavior causes lower compressive yield strength compared with tensile one for extruded AZ31[3–4] and AZ61[5] magnesium alloys. Previous studies also reported the asymmetric stress–strain hysteresis loops in strain-

controlled low cycle fatigue behaviors of extruded magnesium alloys[6–9]. On the other hand, load-controlled high cycle fatigue properties of AZ31 magnesium alloy[3–4, 10–13] and AZ61 magnesium alloy[14–15] were reported. However, the relationships among mechanical properties, fatigue strength and fatigue crack initiation/propagation mechanisms of polycrystalline magnesium alloys are not clear in detail.

The purpose of present study is to investigate the axial tension–compression fatigue behavior (fatigue strength, crack initiation and propagation behavior) of rolled AZ31B magnesium alloy plate.

2 Experimental

Material used in the present study is commercial rolled AZ31B magnesium alloy plate with a thickness of 16 mm. Chemical composition is listed in Table 1. Two types of specimens were machined with the loading axis parallel (L-specimen) and perpendicular (T-specimen) to rolling direction. Fatigue specimens with a gauge length of 10 mm and a diameter of 5 mm were machined as shown in Fig.1. Axial tension–compression fatigue tests were performed on an electro-hydraulic testing machine

(capacity: 9.8 kN) at a stress ratio of $R=\sigma_{\min}/\sigma_{\max}=-1$ and a frequency of 10 Hz at room temperature in air. Here, σ_{\max} and σ_{\min} are the maximum and minimum applied stress, respectively. Crack initiation and small crack growth were monitored with replication technique. After fatigue tests, the fracture surfaces were observed by scanning electron microscope (SEM).

Table 1 Chemical composition of specimens (mass fraction, %)

Al	Zn	Mn	Fe	Si	Cu	Ni	Mg
3.13	0.98	0.35	0.01	0.005	0.004	0.002	Bal.

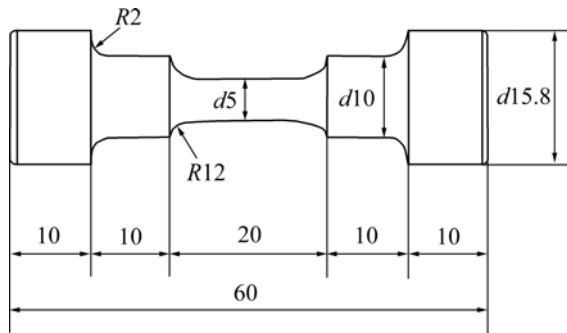


Fig.1 Shape and dimensions of specimen for axial tension–compression fatigue tests (Unit: mm)

3 Results and discussion

3.1 Microstructure and mechanical properties

Fig.2 shows the optical microstructure of the rolled AZ31B magnesium alloy plate. The average grain size of this alloy was approximately 20 μm . SEM-EBSD analysis indicated that this alloy was of typical texture of rolled magnesium alloy; and basal planes are aligned parallel to rolling direction. Mechanical properties of this alloy are summarized in Table 2. Monotonic compressive 0.2% proof stress, tensile strength and tensile elongation were similar for both specimens. On the other hand, monotonic tensile 0.2% proof stress of the L-specimen was slightly higher than that of the T-specimen. Moreover, monotonic compressive 0.2% proof stresses were lower than tensile ones for both specimens.

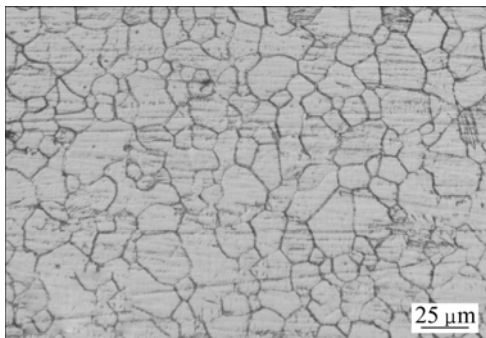


Fig.2 Microstructure of rolled AZ31B magnesium alloy

Table 2 Mechanical properties

Specimen	Compressive 0.2% proof stress, $\sigma_{0.2,comp}/\text{MPa}$	Tensile 0.2% proof stress, $\sigma_{0.2,tens}/\text{MPa}$	Tensile strength, σ_b/MPa	Elongation, $\delta_f/\%$
L-specimen	75	145	253	17.5
T-specimen	76	128	251	16.9

3.2 Fatigue strength

Fig.3 shows S–N (stress amplitude (σ_a)—number of cycles to failure (N)) curves obtained from axial tension–compression fatigue tests. It is well known that fatigue limit does not exist in nonferrous alloys. As can be seen in Fig.3, rolled AZ31B magnesium alloy seemed to possess a definite fatigue limit regardless of specimen direction. Similar S–N curves were also reported in Refs.[3–4, 10–12]. Fatigue strengths (σ_w) of the L- and T-specimens were 95 and 85 MPa, respectively, and the fatigue ratio σ_w/σ_b were 0.38 and 0.34, respectively. The fatigue strength and the fatigue ratio of the L-specimen were higher than those of the T-specimen. In addition, the fatigue lives of the L-specimen were longer than those of the T-specimen in low cycle regime. Moreover, the fatigue strengths were higher than monotonic compressive 0.2% proof stresses. It is emphasized that the fatigue crack does not initiate and propagate even though deformation twins are formed in compressive stress under cyclic tension–compression loading.

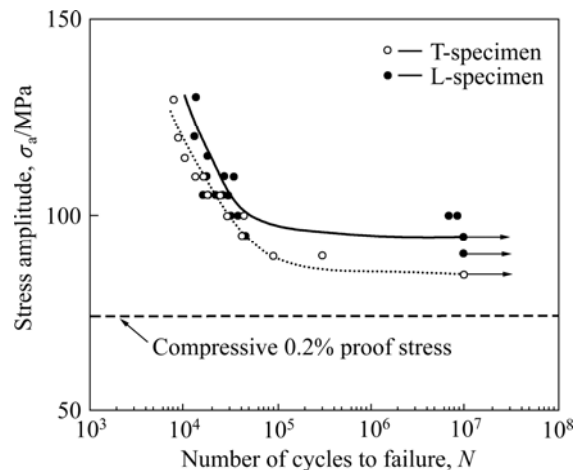


Fig.3 S–N curves of axial tension–compression fatigue tests

3.3 Crack initiation and propagation behavior

Fig.4 shows the surface crack length as a function of cycle ratio N/N_f (N_f : fatigue life) at stress amplitude of 110 MPa. Fatigue crack initiated at early stage of cycle ratio ($N/N_f=0.03$ for the L- and T-specimen) regardless of specimen direction. It was found that the crack length of the T-specimen was longer than that of the L-specimen at the same cycle ratio.

Figs.5 and 6 show the fatigue crack growth behaviors of the L- and T-specimen at stress amplitude of 110 MPa. Figs.5(a) and 6(a) show the crack growth rates as a function of crack tip location. It could be seen that the crack growth rate of the L-specimen was slightly lower than that of the T-specimen. Figs.5(b) and 6(b)

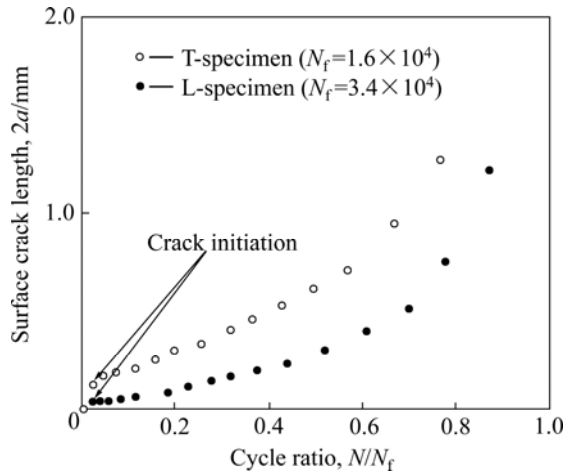


Fig.4 Crack length as function of cycle ratio at $\sigma_a=110$ MPa

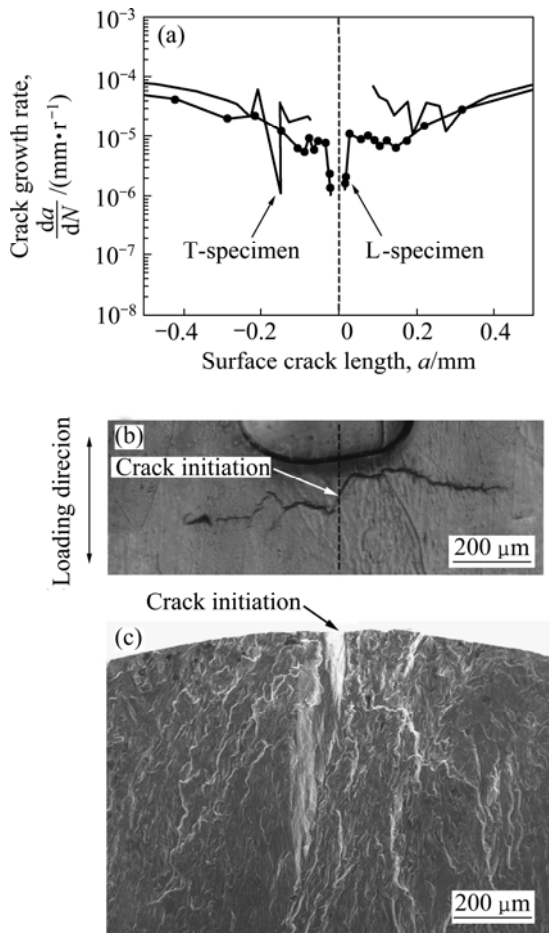


Fig.5 Fatigue crack growth behavior of fatigue tested L-specimen at $\sigma_a=110$ MPa: (a) Crack growth rate; (b) Small crack growth path; (c) Fracture surface

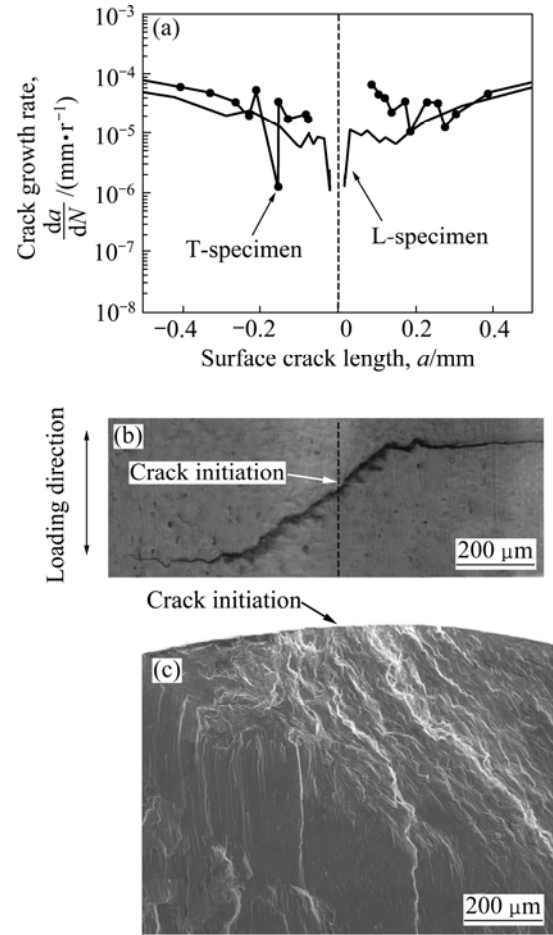


Fig.6 Fatigue crack growth behavior of fatigue tested T-specimen at $\sigma_a=110$ MPa: (a) Crack growth rate; (b) Small crack growth path; (c) Fracture surface

show the fatigue crack path profiles of the specimen surface. The white arrow shows the crack initiation site. After initiation, the fatigue crack path was tilted to 30–45° from the loading axis up to a certain crack length for both specimens. Figs.5(c) and 6(c) show typical SEM images on the fatigue crack initiation site and propagation zone of the fatigue tested specimen. The black arrow shows the crack initiation site. It was found that the fatigue crack initiated at the specimen surface regardless of specimen direction.

Fig.7 shows the typical SEM image on the fatigue crack initiation site of the L-specimen at stress amplitude of 110 MPa. Secondary particle or other defect did not exit at crack initiation site. When the maximum stress amplitude was higher than compressive yield strength, $\{1012\}$ deformation twins were observed on fatigue tested specimen of extruded AZ31 magnesium alloy[3–4]. Moreover, microcracks were found to initiate along twin bands on fatigue tested specimen surface in Ref.[13]. Thus, the deformation twins can play an important role in fatigue crack initiation in fatigue test. This tilted flat surface of the fatigue crack initiation site

has not been identified as the evidence of deformation slip or deformation twin, so further investigation of crystallographic analysis must be required to clarify the relationship between fatigue crack initiation/propagation mechanisms and deformation twins.

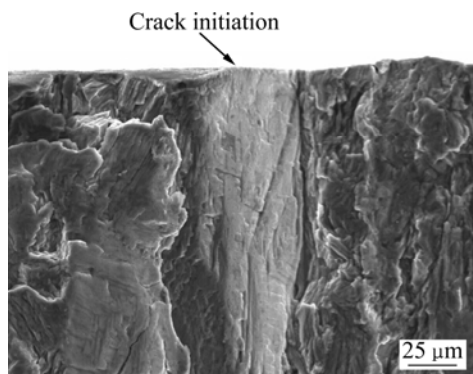


Fig.7 Typical SEM micrograph of crack initiation site of L-specimen at $\sigma_a=110$ MPa

4 Conclusions

1) Fatigue strengths of 10^7 cycles of the L-specimen and the T-specimen were 95 and 85 MPa, respectively. The fatigue strengths were higher than monotonic compressive 0.2% proof stresses.

2) Fatigue lives of the L-specimen were longer than those of the T-specimen in low cycle regime.

3) Fatigue crack initiated at the specimen surface regardless of specimen direction. Fatigue crack growth rate of the L-specimen was lower than that of the T-specimen.

Acknowledgements

The authors would like to thank the IKETANI Science and Technology Foundation and JGC-S Scholarship Foundation for providing financial support.

References

[1] EBERT T, MORDIKE B L. Magnesium: Properties-applications-potential [J]. *Mater Sci Eng A*, 2001, 302(1): 37–45.

- [2] AGNEW S R, MEHROTRA P, LILLO T M, STOICA G M, LIAW P K. Texture evolution of five wrought magnesium alloys during route A equal channel angular extrusion: Experiments and simulations [J]. *Acta Materialia*, 2005, 53(11): 3135–3146.
- [3] SOMEKAWA H, MARUYAMA N, HIROMOTO S, YAMAMOTO A, MUKAI T. Fatigue behaviors and microstructures in extruded Mg-Al-Zn alloy [J]. *Materials Transaction*, 2008, 49(3): 681–684.
- [4] MORITA S, TANAKA S, OHNO N, KAWAKAMI Y, ENJOJI T. Cyclic deformation and fatigue crack behavior of extruded AZ31B magnesium alloy [J]. *Materials Science Forum*, 2010, 638/642: 3056–3061.
- [5] KLEINER S, UGGOWITZER P. J. Mechanical anisotropy of extruded Mg-6%Al-1%Zn alloy [J]. *Mater Sci Eng A*, 2004, 379(1/2): 258–263.
- [6] HASEGAWA S, TSUCHIDA Y, YANO H, MATSUI M. Evaluation of low cycle fatigue life in AZ31 magnesium alloy [J]. *International Journal of Fatigue*, 2007, 29(9/11): 1839–1845.
- [7] LIN X Z, CHEN D L. Strain controlled cyclic deformation behavior of an extruded magnesium alloy [J]. *Mater Sci Eng A*, 2008, 496(1/2): 106–113.
- [8] WU L, JAIN A, BROWN D W, STOICA G M, AGNEW S R, CLAUSEN B, FIELDEN D E, LAIW P K. Twinning-detwinning behavior during the strain-controlled low-cycle fatigue testing of a wrought magnesium alloy, ZK60A [J]. *Acta Materialia*, 2008, 56(4): 688–695.
- [9] MATSUZUKI M, HORIBE S. Analysis of fatigue damage process in magnesium alloy AZ31 [J]. *Mater Sci Eng A*, 2009, 504(1/2): 169–174.
- [10] TOKAJI K, KAMAKURA M, ISHIZUMI Y, HASEGAWA N. Fatigue behaviour and fracture mechanism of a rolled AZ31 magnesium alloy [J]. *International Journal of Fatigue*, 2004, 26(11): 1217–1224.
- [11] OCHI Y, MASAKI K, HIRASAWA T, WU X, MATSUMURA T, TAKIGAWA Y, HIGASHI K. High cycle fatigue property and micro crack propagation behavior in extruded AZ31 magnesium alloys [J]. *Materials Transaction*, 2006, 47(4): 989–994.
- [12] ISHIIHARA S, NAN Z, GOSHIMA T. Effect of microstructure on fatigue behavior of AZ31 magnesium alloy [J]. *Mater Sci Eng A*, 2007, 468/470: 214–222.
- [13] YANG F, YIN S M, LI S X, ZHANG Z F. Crack initiation mechanism of extruded AZ31 magnesium alloy in the very high cycle fatigue regime [J]. *Mater Sci Eng A*, 2008, 491(1/2): 131–136.
- [14] SHIH T S, LIU W S, CHEN Y J. Fatigue of as-extruded AZ61A magnesium alloy [J]. *Mater Sci Eng A*, 2002, 325(1/2): 152–162.
- [15] SAJURI Z B, MIYASHITA Y, HOSOKAWA Y, MUTOH Y. Effects of Mn content and texture on fatigue properties of as-cast and extruded AZ61 magnesium alloys [J]. *International Journal of Mechanical Sciences*, 2006, 48(2): 198–209.

(Edited by LIU Hua-sen)